Ceramics International 42 (2016) 12838–12842

Contents lists available at ScienceDirect

Ceramics International

journal homepage: www.elsevier.com/locate/ceramint

Influence of Eu and Sr co-substitution on multiferroic properties of $BiFeO_3$

Weiwei Mao [a,b,c], Wei Chen [a,b,c], Xingfu Wang [a,b,c], Yiyi Zhu [a,c], Yuhui Ma [a,c], Hongtao Xue [b,c], Liang Chu [b,c], Jianping Yang [b,c], Xing'ao Li [a,c,*], Wei Huang [a,c,*]

[a] Key Laboratory for Organic Electronics & Information Displays (KLOEID), Institute of Advanced Materials (IAM), School of Materials Science and Engineering (SMSE), Nanjing University of Posts and Telecommunications (NUPT), Nanjing 210023, PR China
[b] College of Science, Information Physics Research Center, Advanced Energy Technology Center, Nanjing University of Posts and Telecommunications (NUPT), Nanjing 210023, PR China
[c] Key Laboratory of Flexible Electronics (KLOFE) & Institute of Advanced Materials (IAM), National Synergistic Innovation Center for Advanced Materials (SICAM), Nanjing Tech University (NanjingTech), 30 South Puzhu Road, Nanjing 211816, PR China

ARTICLE INFO

Article history:
Received 4 March 2016
Received in revised form
20 April 2016
Accepted 7 May 2016
Available online 9 May 2016

Keywords:
$BiFeO_3$
Ferroelectric properties
Magnetic properties
Sol-gel method

ABSTRACT

Pure $BiFeO_3$ (BFO), and Eu-Sr co-substituted BFO samples were prepared by a sol–gel method. The effects of Eu and Sr codoped on the structural, morphological, magnetic and ferroelectric properties were systematically investigated. The X-ray diffraction and Fourier transform infrared spectroscopy reveal that substitution of Eu and Sr at the Bi site results in structural change and single phase formation. The maximum remnant magnetization of 0.287 emu/g and coercive field of 10.305 kOe are observed in the $Bi_{0.85}Eu_{0.05}Sr_{0.10}FeO_3$ sample. The suppression of spin cycloid caused from the structural distortion can play an important role in the improvement of magnetic properties. The Eu and Sr co-doped samples also exhibit good ferroelectric properties, which may be attributed to suppressing the formation of oxygen vacancies by Eu substitution.

1. Introduction

As one of novel compounds, multiferroic materials have attracted significant attention due to the coupled magnetic, ferroelectric, and ferroelastic orders [1]. The interest in these materials is driven by the prospect to control charges by applied magnetic fields and spins by applied voltages. Accordingly, they have been employed in various multifunctional devices such as transducers, multiple-state memories, and spintronics [2–5]. Among all multiferroic materials studied so far, $BiFeO_3$ (BFO) is known to the only single-phase room temperature multiferroic materials, which has simultaneous ferroelectric ($T_C \sim 1103$ K) and G-type antiferromagnetic ($T_N \sim 643$ K) properties above room temperature [6]. The unique multiferroic behavior permits BFO to be an ideal candidate for most important multifunctional applications [7–10]. Though this property is very promising in terms of practical applications, the magnetic ordering is of antiferromagnetic type with a spatially modulated spin structure, which net magnetization is forbidden and inhibits the observation of the linear magnetoelectric effect meanwhile [11]. Moreover, it is usually difficult to obtain saturated ferroelectric hysteresis loops from the pure BFO at room temperature due to the high leakage current resulting from some defects, such as oxygen vacancies, secondary phase and interfacial quality [12–14].

The physical properties of a material could be modulated by the process of ions doping. In order to reduce the leakage current and enhance the magnetic properties, several studies have been made to control the structure distortion of BFO by substituting Bi^{3+} with rare earth ions [15–17]. For instance, Eu-doped BFO films have been grown by pulsed laser deposition with superior magnetic and ferroelectric properties [18]. These significantly improved ferroelectric properties could be attributed to the lower leakage current after doping, while the enhanced ferromagnetism might be ascribed to the substitution-induced suppression of the spiral spin modulation. It has also been studied the Eu-doped BFO polycrystalline ceramics by a solid state reaction method [19]. Eu substitution induced the enhanced remnant magnetization due to the ferromagnetic coupling between Eu^{3+} and Fe^{3+} ions. Moreover, some research groups have tried to substitute Bi site by alkaline earth metals, including Ba, Ca, Sr, etc., to improve the magnetic properties of BFO [20–23]. Recently, improved magnetic

* Corresponding authors at: Key Laboratory for Organic Electronics & Information Displays (KLOEID), Institute of Advanced Materials (IAM), School of Materials Science and Engineering (SMSE), Nanjing University of Posts and Telecommunications (NUPT), Nanjing 210023, PR China.
E-mail addresses: lxahbmy@126.com (X. Li), iamwhuang@njupt.edu.cn (W. Huang).

http://dx.doi.org/10.1016/j.ceramint.2016.05.048
0272-8842/

and ferroelectric properties were found in BFO co-substituted with rare earth ions and alkaline earth ions. Naeimi et al. have reported the significant enhancement of the remnant magnetization by co-doping of Ba and Er into BFO, which may be due to the collapse of spin structure and modifying exchange interactions because of Er [24]. Cheng et al. have found a structural phase transition of rhombohedral-to-cubic occurs in $Bi_{0.75}Pr_{0.15}Ba_{0.1}Fe_3$ sample [25]. The strong enhancement of the spontaneous magnetization is significantly affected by the local lattice distortion and collapse of the spatial spin structure in the Pr-Ba co-substituted sample. Quan et al. have synthesized Ca and Nd co-doped BFO through a sol–gel method [26]. The co-doped samples showed relatively low current leakage density and higher ferromagnetic properties compared with Ca-doped BFO. According to our knowledge, there is no other reports giving the synthesis of Eu and Sr co-doped BFO. Therefore, the aim of the present work is to synthesize Eu and Sr co-doped BFO using a sol-gel method and to uncover the influence of the structural, morphological, magnetic and ferroelectric properties from Eu and Sr co-substitution.

2. Experimental

Pure BFO and $Bi_{0.95-x}Eu_{0.05}Sr_xFeO_3$ (x=0, 0.05 and 0.10) samples were prepared by a sol–gel method. Appropriate amount of Bi_2O_3, $Fe(NO_3)_3 \cdot 9\ h_2O$, Eu_2O_3 and SrO with suitable stoichiometry were dissolved in dilute nitric acid and distilled water. Tartaric acid, with the amount of the total metallic ions in the precursor solution, was added as chelating agents. Then the mixed solution was stirred for several hours to form a homogeneous gel. Finally, the gel was dried at 80 °C for 48 h and calcined at 550 °C for 2 h.

The phase purity and crystal structure of calcined powders were examined using X-ray diffraction (XRD) (Bruker D8 Advance X-ray diffractometer) with Cu-Kα radiation. The morphology was examined using scanning electron microscopy (SEM, JEOL-6380LV, Japan). Fourier Transform Infrared Spectroscopy (FT-IR) measurements were carried out on Fourier Transform Infrared spectrometer (Model: IRPrestige-21). Magnetization responses of all the samples were examined by measuring the magnetization hysteresis curves using a superconducting quantum interference device (SQUID) magnetometer. The ferroelectric hysteresis loops (*P*–*E*) and leakage current density–electric field (*J*–*E*) curves were measured using Radiant precision materials analyzer with each powder sample pressed into thin piece under a pressure of 20 MPa having an area around 0.2 cm^2 and a thickness around 0.08 cm. Ag electrodes were coated on both sides.

3. Results and discussion

Fig. 1(a) shows the typical XRD patterns of all the samples at room temperature. All the diffraction peaks associated with the pure BFO are well matched with the rhombohedral structure (JCPDS file No. 71-2494). There is no obvious secondary phases in XRD patterns of doped-BFO, while a negligible impurity phase (marked with "*") was observed in pure BFO. The absence of the oxides of Eu or Sr diffraction peaks implies that substitution did not trigger the formation of the impurity phases, thereby means that Eu and Sr ions have doped into BFO cell successfully. Fig. 1 (b) shows the magnified XRD patterns in the range of 2θ from 31° to 33°, which reveals the evolution of the (104) and (110) diffraction peaks by doping. For x=0, the two peaks shift slightly toward higher angle. Thus, based on the Bragg's law the unit cell volume decrease by only Eu doping, which may be due to the smaller ionic radius of Eu^{3+} compared with Bi^{3+}. After doping with Sr, the two peaks shift toward lower angle for the samples with x=0.05 and 0.10, which indicates that Sr substitution leads to an increase in the unit cell volume because of the Sr^{2+} with a bigger ionic radius than Bi^{3+} [19,27]. After doping with Sr, the two peaks shift toward lower angle which can be attributed to the Sr^{2+} ion with a bigger ionic radius than Bi^{3+} ion [28,29]. The split peaks become weak in the sample with Sr doping concentration of 10%, which indicates that the higher doping concentration of Sr induces greater structural distortion.

The surface morphological characteristics of all the samples were investigated using SEM, which are shown in Fig. 2. For pure BFO, the particles display rather irregular and agglomerate, the range of grain size is about 150–1200 nm. It is observed that the

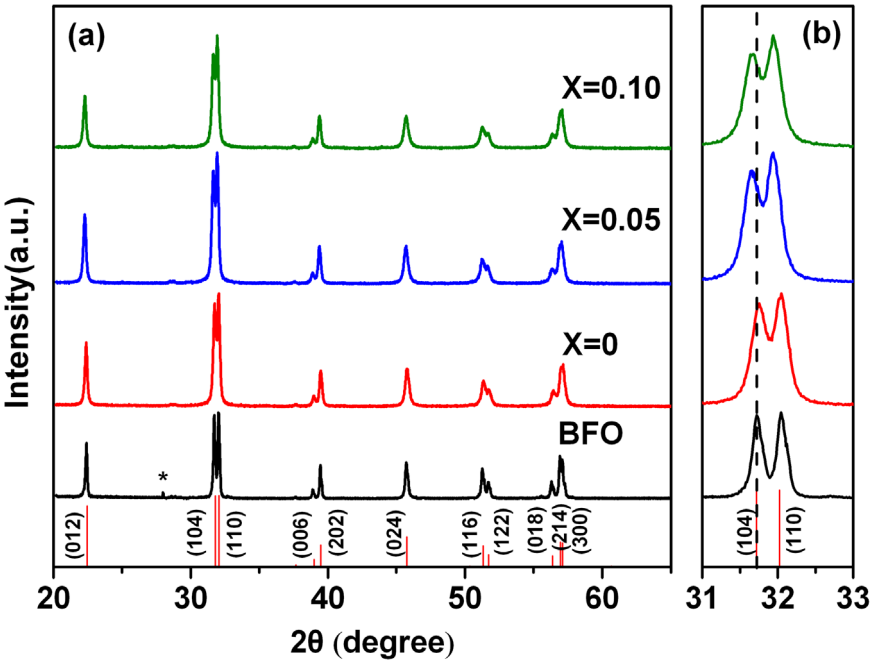

Fig. 1. (a) X-ray diffraction patterns of all the samples at room temperature. (b) Enlarged view of the diffraction peaks (104) and (110).

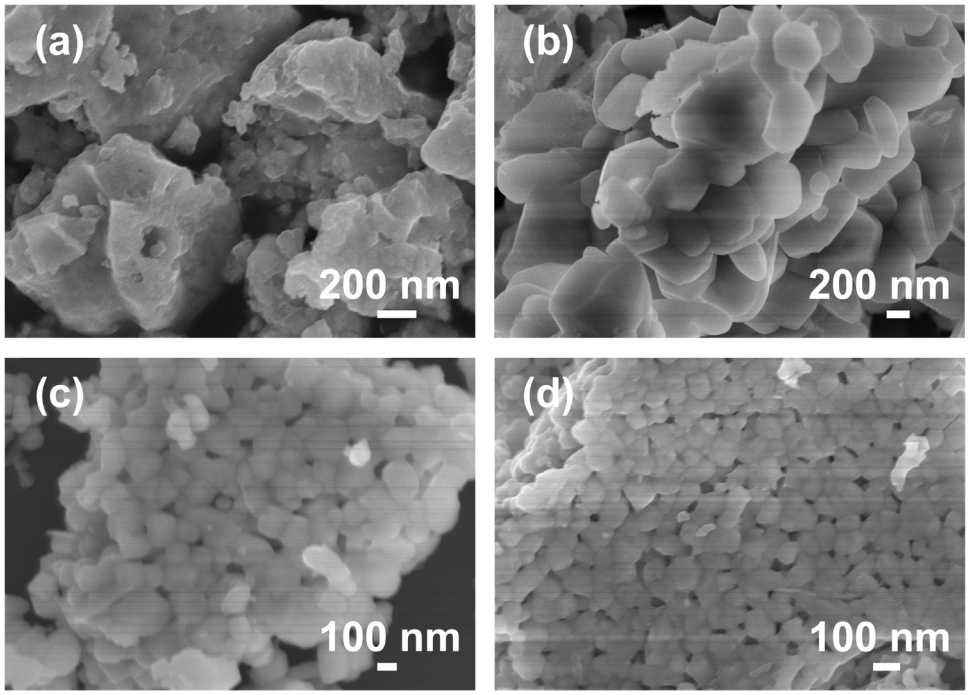

Fig. 2. SEM images for (a) BFO, (b) x=0, (c) x=0.05, and (d) x=0.10 samples.

grain size for x=0 sample decreases to 150–800 nm. As can be seen in Fig. 2(c)–(d), the doping of Sr has obvious effect on morphology and size of BFO sample. Sr dopant homogenizes the morphology of the particles and gives rise to a granular microstructure with nearly spherical shape, although the particles are still seriously agglomerate. Furthermore, the grain size is remarkably reduced by Sr doping. For x=0.05 samples, uniform particles with the diameter from 100 to 300 nm can be found in Fig. 2(c). The grain size changes little when increase the doped content to 10%, which is about 80–200 nm. It is observed that the grain size decreases obviously for the x=0.05 and 0.10 samples, which may be due to the inhibition of grain growth caused by the substitution of Sr [30].

Details of the structure evolution with ion substitution on BFO can be also expressed through FT-IR spectra. FT-IR spectra of all the samples are shown in Fig. 3 in the wave number range of 400–1500 cm^{-1}. Typical band characteristics of metal oxygen bonds are observed in the range of 400–600 cm^{-1}. The characteristic peaks at around 550 cm^{-1} and 450 cm^{-1} are, respectively, assigned to Fe–O bond stretching and O–Fe–O bending of FeO6 group in the perovskite structure. These modes are consistence with the previously reported data [22,31,32]. With the increase in substitution concentration, these two absorption peaks shift to the lower wave number side. This result indicates that Eu and Sr co-substitution has obvious influence on the Fe–O octahedron in BFO, which has also been observed in other similar materials [33].

Fig. 4 shows the magnetic hysteresis (*M-H*) loops at room temperature for all the samples with a maximum applied magnetic field of 70 kOe. And magnetic parameters have been enlisted in Table 1. It is clearly seen that pure BFO exhibits nearly linear *M-H* loop with small values of remnant magnetization (*Mr*~0.006 emu/g) and coercive field (*Hc*~0.879 kOe), which suggests that pure BFO is antiferromagnetic. Compared with BFO, there is a narrow hysteresis loop of x=0 sample with higher values of *Mr* (~0.040 emu/g) and *Hc* (~2.207 kOe). With the increasing content of x, the obvious hysteresis loops are observed from x=0.05 and 0.10 samples. And the highest values of *Mr*

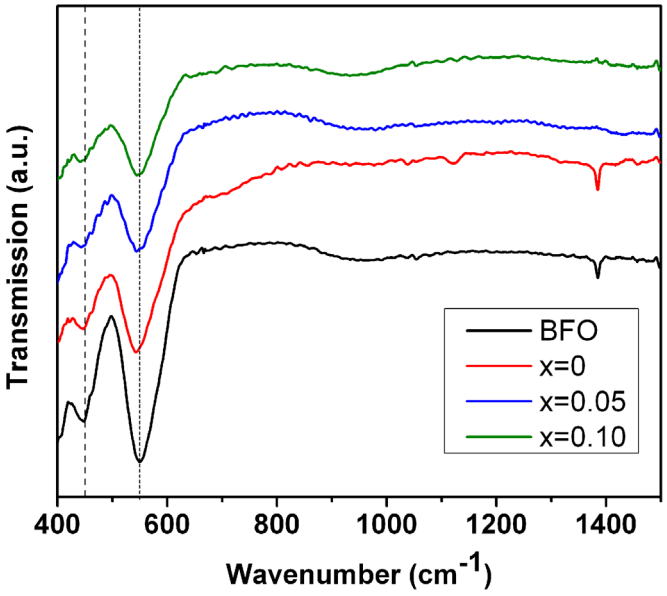

Fig. 3. FT-IR spectra of all the samples.

(~0.287 emu/g) and *Hc* (~10.305 kOe) can be obtained from x=0.1 sample. As known, BFO is a G-type antiferromagnetic, and nearest neighbour Fe magnetic moments are aligned antiparallel to each other. But the antiferromagnetic Fe sublattices are not aligned perfectly due to the Dzyaloshinskii–Moriya exchange interaction, as a result of a weak ferromagnetism, which is macroscopically cancelled by a spiral spin structure of long period (62 nm) [11,34]. The results of the XRD and FT-IR revealed that substitution caused internal structure distortion related to changes in Fe–O bond distances and bond angles. The enhancement in magnetization may be induced by the structural distortion, which enhanced suppression of the spin cycloid by increasing Sr-doping content in BFO [35–37].

The plots of the leakage current density (*J*) versus the applied electric field (*E*) of all the samples were measured at room

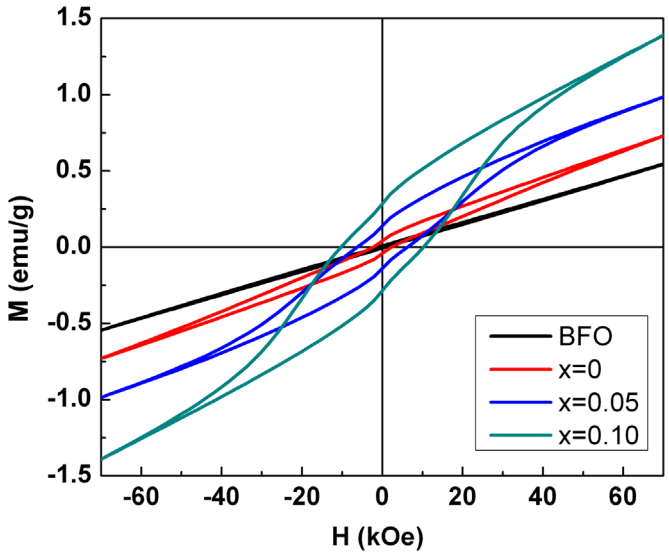

Fig. 4. Room temperature magnetic hysteresis loops for all the samples.

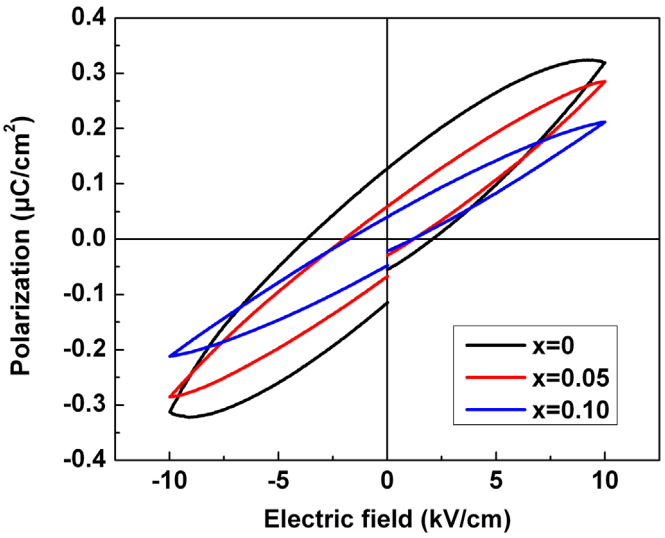

Fig. 6. Polarization hysteresis loops for x=0, x=0.05 and x=0.10 samples measured at room temperature.

Table 1
Magnetic parameters of all the samples.

	Maximum magnetization (emu/g)	Remnant magnetization (emu/g)	Coercive field (kOe)
BFO	0.544	0.006	0.879
x=0	0.730	0.040	2.207
x=0.05	0.986	0.138	6.268
x=0.10	1.391	0.287	10.305

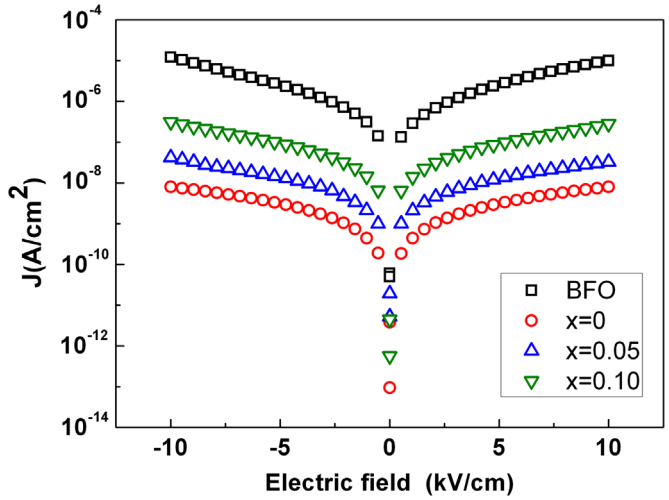

Fig. 5. Room temperature leakage current density-electric field behaviors of all the samples.

temperature as shown in Fig. 5. It is seen that the pure BFO has a higher leakage current compared with the doped samples, which implies the leakage current can be reduced by substitution. Moreover, the leakage current densities are increased with increasing the substitution content of Sr, and current densities are 7.98×10^{-9} A/cm^2 (x=0), 3.29×10^{-8} A/cm^2 (x=0.05) and 2.83×10^{-7} A/cm^2 (x=0.10) at maximum applied electric field of 10 kV/cm, respectively. As known to all, the origin of the high leakage current and low resistance in BFO is mainly attributed to the defects such as secondary phases or oxygen vacancies [12]. Previous works confirmed that doping of rare earth ions can suppress the formation of oxygen vacancies in BFO cell [38,39]. Hence, doping of Eu can decrease the leakage current of BFO. However, the creation of oxygen vacancies to neutralize the charge produced by the substituting Sr^{2+} for Bi^{3+} [40,41]. So the leakage current increase monotonically with the increase of the Sr content.

In order to study the ferroelectric behavior of the doped samples, the polarization hysteresis (*P-E*) loops were measured under an applied electric field (*E*) of 10 kV/cm, which are shown in Fig. 6. All the samples exhibit unsaturated characteristics even under large electric field, which indicate that they are ferroelectric but having lossy loop behavior. The lossy features of those samples can be related to the leakage current. For x=0 sample, the best ferroelectric hysteresis loop is observed with a remnant polarization (*Pr*) of 0.313 μC/cm^2 and a coercive electric field (*Ec*) of 0.115 kV/cm. With increasing substitution concentration of Sr (x=0.05), both *Pr* and *Ec* values decrease to 0.285 μC/cm^2 and 0.068 kV/cm, respectively. On further increase the doping content of Sr (x=0.10), *Pr* value decreases to 0.212 μC/cm^2 and *Ec* to 0.048 kV/cm under the same applied electric field of 10 kV/cm, which is due to the lower resistivity and higher leakage current. It can be seen from the *J-E* curves (Fig. 5), the doping of Sr induced oxygen vacancies in BFO, thereby increased the leakage current density. For x=0 sample, Eu substitution can reduce leakage current density of BFO, and therefore enhance ferroelectric behavior [18,42].

4. Conclusion

In summary, single-phase Eu and Sr co-doped BFO samples were prepared by a sol-gel method. The XRD and FT-IR results show the structural distortion caused by the doping. The size and morphology of the particles have been confirmed using SEM. The suppression of spin cycloid due to the structural distortion has been found, which could enhance the magnetic properties. In addition, the doping of Eu into BFO plays an important role in reducing the leakage current and enhancing the ferroelectric properties. All these results suggest that appropriate co-substitution with Eu and Sr is effective in enhancing the multiferroic properties of the BFO, which are essential for practical applications.

Acknowledgements

We acknowledge the financial support from the Ministry of Education of China (No. IRT1148), Jiangsu Synergistic Innovation Center for Advanced Materials (SICAM), the Project Funded by the Priority Academic Program Development of Jiangsu Higher Education Institutions (PAPD, YX03001), the National Natural Science Foundation of China (51372119, 61377019, 61136003, 51173081), College Postgraduate Research and Innovation Project of Jiangsu Province (KYLX_0794, KYLX15_0848), the Natural Science Foundation of Jiangsu (KZ0070715050), the Seed Project Funded by Introducing Talent of NJUPT (XK0070915022) and the Natural Science Foundation of NJUPT (NY214129, NY214130, NY214181, NY215176).

References

[1] Y. Tokura, S. Seki, N. Nagaosa, Multiferroics of spin origin, reports on progress in physics, Phys. Soc. 77 (2014) 076501.
[2] W. Eerenstein, N.D. Mathur, J.F. Scott, Multiferroic and magnetoelectric materials, Nature 442 (2006) 759–765.
[3] S.W. Cheong, M. Mostovoy, Multiferroics: a magnetic twist for ferroelectricity, Nat. Mater. 6 (2007) 13–20.
[4] C.S. Watson, C. Hollar, K. Anderson, W.B. Knowlton, P. Müllner, Magneto-mechanical four-state memory, Adv. Funct. Mater. 23 (2013) 3995–4001.
[5] J. Ma, J. Hu, Z. Li, C.W. Nan, Recent progress in multiferroic magnetoelectric composites: from bulk to thin films, Adv. Mater. 23 (2011) 1062–1087.
[6] J. Wang, J.B. Neaton, H. Zheng, V. Nagarajan, S.B. Ogale, B. Liu, D. Viehland, V. Vaithyanathan, D.G. Schlom, U.V. Waghmare, N.A. Spaldin, K.M. Rabe, M. Wuttig, R. Ramesh, Epitaxial $BiFeO_3$ multiferroic thin film heterostructures, Science 299 (2003) 1719–1722.
[7] B. Sun, L. Wei, H. Li, P. Chen, White-light-controlled ferromagnetic and ferroelectric properties of multiferroic single-crystalline $BiFeO_3$ nanoflowers at room temperature, J. Mater. Chem. C 2 (2014) 7547–7551.
[8] X. Wang, W. Mao, J. Zhang, Y. Han, C. Quan, Q. Zhang, T. Yang, J. Yang, Xa Li, W. Huang, Facile fabrication of highly efficient g-C_3N_4/$BiFeO_3$ nanocomposites with enhanced visible light photocatalytic activities, J. Colloid Interface Sci. 448 (2015) 17–23.
[9] R. Guo, L. You, Y. Zhou, Z.S. Lim, X. Zou, L. Chen, R. Ramesh, J. Wang, Non-volatile memory based on the ferroelectric photovoltaic effect, Nat. Commun. 4 (2013) 1990.
[10] Y. Li, X. Liu, Y. Sun, S. Sheng, H. Liu, P. Yang, S. Yang, Enhanced photovoltaic effect in K substituted $BiFeO_3$ films, J. Alloy. Compd. 644 (2015) 602–606.
[11] I. Sosnowska, T.P. Neumaier, E. Steichele, Spiral magnetic ordering in bismuth ferrite, J. Phys. C: Solid State Phys. 15 (1982) 4835–4846.
[12] X. Qi, J. Dho, R. Tomov, M.G. Blamire, J.L. MacManus-Driscoll, Greatly reduced leakage current and conduction mechanism in aliovalent-ion-doped $BiFeO_3$, Appl. Phys. Lett. 86 (2005) 2903.
[13] W. Mao, X. Wang, Y. Han, Xa Li, Y. Li, Y. Wang, Y. Ma, X. Feng, T. Yang, J. Yang, W. Huang, Effect of Ln (Ln=La, Pr) and Co co-doped on the magnetic and ferroelectric properties of $BiFeO_3$ nanoparticles, J. Alloy. Compd. 584 (2014) 520–523.
[14] T. Wang, S. Song, M. Wang, J. Li, M. Ravi, Effect of annealing atmosphere on the structural and electrical properties of $BiFeO_3$ multiferroic ceramics prepared by sol–gel and spark plasma sintering techniques, Ceram. Int. 42 (2016) 7328–7335.
[15] G. Dong, G. Tan, Y. Luo, W. Liu, H. Ren, A. Xia, Investigation of Tb-doping on structural transition and multiferroic properties of $BiFeO_3$ thin films, Ceram. Int. 40 (2014) 6413–6419.
[16] H. Liu, T. Liu, X. Wang, Study on the ferroelectricity of Eu substituted $BiFeO_3$ films, Solid State Commun. 149 (2009) 1958–1961.
[17] P. Thakuria, P.A. Joy, High room temperature ferromagnetic moment of Ho substituted nanocrystalline $BiFeO_3$, Appl. Phys. Lett. 97 (2010) 162504.
[18] Z. Hu, M. Li, J. Liu, L. Pei, J. Wang, B. Yu, X. Zhao, Structural transition and multiferroic properties of eu-doped $BiFeO_3$ thin films, J. Am. Ceram. Soc. 93 (2010) 2743–2747.
[19] P.C. Sati, M. Kumar, S. Chhoker, M. Jewariya, Influence of Eu substitution on structural, magnetic, optical and dielectric properties of $BiFeO_3$ multiferroic ceramics, Ceram. Int. 41 (2015) 2389–2398.
[20] S. Chauhan, M. Kumar, S. Chhoker, S. Katyal, M. Jewariya, B. Suma, G. Kunte, Structural modification and enhanced magnetic properties with two phonon modes in Ca–Co codoped $BiFeO_3$ nanoparticles, Ceram. Int. 41 (2015) 14306–14314.
[21] B. Ramachandran, A. Dixit, R. Naik, G. Lawes, M.S. Ramachandra Rao, Dielectric relaxation and magneto-dielectric effect in polycrystalline $Bi_{0.9}Ca_{0.1}FeO_{2.95}$, Appl. Phys. Lett. 100 (2012) 252902.
[22] S. Chauhan, M. Arora, P.C. Sati, S. Chhoker, S.C. Katyal, M. Kumar, Structural, vibrational, optical, magnetic and dielectric properties of $Bi_{1-x}Ba_xFeO_3$ nanoparticles, Ceram. Int. 39 (2013) 6399–6405.
[23] V.A. Khomchenko, D.A. Kiselev, J.M. Vieira, A.L. Kholkin, M.A. Sa, Y. G. Pogorelov, Synthesis and multiferroic properties of $Bi_{0.8}A_{0.2}FeO_3$ (A=Ca,Sr, Pb) ceramics, Appl. Phys. Lett. 90 (2007) 242901.
[24] A.S. Naeimi, E. Dehghan, D. Sanavi Khoshnoud, A. Gholizadeh, Enhancment of ferromagnetism in Ba and Er co-doped $BiFeO_3$ nanoparticles, J. Magn. Magn. Mater. 393 (2015) 502–507.
[25] G.F. Cheng, Y.H. Huang, J.J. Ge, B. Lv, X.S. Wu, Effects of local structural distortion on magnetization in $BiFeO_3$ with Pr, Ba co-doping, J. Appl. Phys. 111 (2012) 07C707.
[26] C. Quan, Y. Ma, Y. Han, X. Tang, M. Lu, W. Mao, J. Zhang, J. Yang, Xa Li, W. Huang, Effect of Nd substitution for Ca on crystal structure, optical and magnetic properties of multiferroic $Bi_{0.9}Ca_{0.1}FeO_3$, J. Alloy. Compd. 635 (2015) 272–277.
[27] J. Liu, L. Fang, F. Zheng, S. Ju, M. Shen, Enhancement of magnetization in Eu doped $BiFeO_3$ nanoparticles, Appl. Phys. Lett. 95 (2009) 022511.
[28] Y. Niu, J. Sunarso, W. Zhou, F. Liang, L. Ge, Z. Zhu, Z. Shao, Evaluation and optimization of $Bi_{1-x}Sr_xFeO_{3-\delta}$ perovskites as cathodes of solid oxide fuel cells, Int. J. Hydrog. Energy 36 (2011) 3179–3186.
[29] C. Ostos, O. Raymond, N. Suarez-Almodovar, D. Bueno-Baqués, L. Mestres, J. M. Siqueiros, Highly textured Sr, Nb co-doped $BiFeO_3$ thin films grown on $SrRuO_3$/Si substrates by rf- sputtering, J. Appl. Phys. 110 (2011) 024114.
[30] K. Saravana Kumar, C. Venkateswaran, D. Kannan, B. Tiwari, M.S. Ramachandra Rao, Mechanical milling assisted synthesis of Ba–Mn co-substituted $BiFeO_3$ ceramics and their properties, J. Phys. D: Appl. Phys. 45 (2012) 415302.
[31] R.K. Mishra, D.K. Pradhan, R.N.P. Choudhary, A. Banerjee, Effect of yttrium on improvement of dielectric properties and magnetic switching behavior in $BiFeO_3$, J. Phys.: Condens. Matter 20 (2008) 045218.
[32] V.M. Gaikwad, S.A. Acharya, Investigation of spin phonon coupling in $BiFeO_3$ based system by Fourier transform infrared spectroscopy, J. Appl. Phys. 114 (2013) 193901.
[33] G. Rojas-George, J. Silva, R. Castañeda, D. Lardizábal, O.A. Graeve, L. Fuentes, A. Reyes-Rojas, Modifications in the rhombohedral degree of distortion and magnetic properties of Ba-doped $BiFeO_3$ as a function of synthesis methodology, Mater. Chem. Phys. 146 (2014) 73–81.
[34] D.P. Dutta, B.P. Mandal, R. Naik, G. Lawes, A.K. Tyagi, Magnetic, Ferroelectric, and Magnetocapacitive Properties of Sonochemically Synthesized Sc-Doped $BiFeO_3$ Nanoparticles, J. Phys. Chem. C 117 (2013) 2382–2389.
[35] W. Mao, Xa Li, Y. Li, X. Wang, Y. Wang, Y. Ma, X. Feng, T. Yang, J. Yang, Structural phase transition and multiferroic properties of single-phase $Bi_{1-x}Er_xFe_{0.95}Co_{0.05}O_3$, Mater. Lett. 97 (2013) 56–58.
[36] S. Vijayasundaram, G. Suresh, R. Mondal, R. Kanagadurai, Substitution-driven enhanced magnetic and ferroelectric properties of $BiFeO_3$ nanoparticles, J. Alloy. Compd. 658 (2016) 726–731.
[37] X. Yan, G. Tan, W. Liu, H. Ren, A. Xia, Structural, electric and magnetic properties of Dy and Mn co-doped $BiFeO_3$ thin films, Ceram. Int. 41 (2015) 3202–3207.
[38] W. Mao, X. Wang, L. Chu, Y. Zhu, Q. Wang, J. Zhang, J. Yang, Xa Li, W. Huang, Simultaneous enhancement of magnetic and ferroelectric properties in Dy and Cr co-doped $BiFeO_3$ nanoparticles, Phys. Chem. Chem. Phys. 18 (2016) 6399–6405.
[39] N. Jeon, D. Rout, I.W. Kim, S.-J.L. Kang, Enhanced multiferroic properties of single-phase $BiFeO_3$ bulk ceramics by Ho doping, Appl. Phys. Lett. 98 (2011) 072901.
[40] H. Chang, F. Yuan, K. Tu, Y. Lo, S. Tu, C. Wang, A. Yang, C. Tu, S. Jen, W. Chang, Effect of Ba substitution on the multiferroic properties of $BiFeO_3$ films on glass substrates, J. Appl. Phys. 117 (2015) 17C734.
[41] R. Dahiya, A. Agarwal, S. Sanghi, A. Hooda, P. Godara, Structural, magnetic and dielectric properties of Sr and V doped $BiFeO_3$ multiferroics, J. Magn. Magn. Mater. 385 (2015) 175–181.
[42] X. Zhang, Y. Sui, X. Wang, Y. Wang, Z. Wang, Effect of Eu substitution on the crystal structure and multiferroic properties of $BiFeO_3$, J. Alloy. Compd. 507 (2010) 157–161.